ELSEVIER

Chemical Engineering Journal 65 (1997) 165–174

Chemical Engineering Journal

Effect of sinusoidal perturbations of feed concentration on multi-substrate carbon oxidation and nitrification process in an upflow packed-bed biofilm reactor

Shafkat A. Beg *, Mirza M. Hassan, Muhammad A.S. Chaudhry

Department of Chemical Engineering, King Fahd University of Petroleum and Minerals, Dhahran 31261, Saudi Arabia

Received 14 November 1995; accepted 7 March 1997

Abstract

The performance of an upflow packed bed biofilm reactor has been analyzed under multi-substrate limitation by considering simultaneous carbon oxidation and nitrification reactions. For an inlet concentration of 200 mg l^{-1} of NH_4^+–N and 50 mg l^{-1} of methanol, the results show that organic substrate is consumed very rapidly near the inlet of the reactor while most of the NH_4^+–N is converted in the central region of the reactor. When the inlet concentration of methanol is subjected to sinusoidal variation, the exit concentration of NH_4^+–N also follows a sinusoidal pattern although its inlet concentration was subjected to step input. However, the methanol exit concentration exhibits the typical step input response when the inlet NH_4^+–N concentration is subjected to sinusoidal variation. The concentration profiles within the biofilm reactor show that oxygen is a limiting component at the middle of the reactor when both methanol and NH_4^+–N inlet concentrations follow sinusoidal variation. © 1997 Elsevier Science S.A.

Keywords: Upflow packed bed biofilm reactor; Submerged biofilters; Simultaneous carbon oxidation and nitrification; Biological wastewater treatment

1. Introduction

A number of biological, chemical and physical processes have been developed for the removal of nitrogen from wastewaters. Biological nitrification has long been recognized as an efficient means of ammonia removal from soil, wastewaters, rivers and lakes. It also has the advantages of process stability and economic feasibility. Moreover, nitrification has been extensively studied and continues to be of interest to microbiologists, engineers and biochemists and several comprehensive reviews have been published on these aspects [1–9].

The nitrification process contributes to nitrogen removal by transforming ammonia to more oxidized nitrogen compounds such as nitrite or nitrate which are readily converted to nitrogen gas in the denitrification process that follows nitrification. Nitrification by a biofilm or by freely suspended cells separated from or combined with organic degradation is commonly employed. The attached-growth or biofilm reactors show a higher nitrogen removal efficiency and have several advantages: low operating cost, simplicity of operation, absence of sludge recycle, low sludge production and no washout problem etc. Heightened interest in the application of attached growth systems has emerged since the 1960s with the development of more efficient plastic support media for biological growth which allows construction of smaller treatment units, thereby reducing process cost.

2. Review of literature

2.1. Modelling of simultaneous carbon oxidation and nitrification

In addition to the nitrification process alone, the combined organic oxidation and nitrification process has also been carried out successfully in both suspended- and attached-growth processes. These operating options are possible because of the physiological difference in the bacteria responsible for these oxidations. However, the yield of new cell material is much lower for nitrifiers than it is for organic oxidizers. Because of the lower yield, nitrifiers also have much lower maximum specific growth rate, which means that under conditions conducive to both type of microorganisms, heterotrophs will grow and accumulate much faster than the

* Corresponding author. Fax: +966 3 860 4234; E-mail: sabeg@dpc.kfupm.edu.sa

PII S1385-8947(97)00022-3

autotrophs can. As a result, nitrification in attached-growth systems occurs after the organic carbon concentration falls low enough to limit the growth of heterotrophs so that the nitrifiers can compete for space in the oxygenated zones of the biofilm. Thus carbon oxidation occurs at the influent end of a trickling filter and rotating biological contactor systems, while nitrification takes place near the effluent end after the BOD level has fallen to less than about 25 mg l^{-1} [10–15].

The development of mathematical models to describe the observed behaviour in a biofilm reactor carrying out both organic oxidation and nitrification reactions has also received attention during the last decade. Harremoes [16] presented a simplified model for organic oxidation and nitrification in a mixed microbial film in which zero-order kinetics was assumed for both heterotrophs and autotrophs and the nitrifying population increased exponentially with biofilm depth. However, the use of zero order heterotrophic kinetics is unlikely since the half saturation constant (50 mg COD l^{-1}) is comparable to the COD concentration at the biofilm surface in the treatment of sewage (30–200 mg l^{-1}). The use of zero order kinetics therefore leads to an underestimation of the depth of the heterotrophic layer and an overestimation of the ammonium flux.

Strand [17] analysed the oxidation of organic carbon and ammonium–nitrogen in aerobic biofilms and presented a simplified model consisting of uniform layers of heterotrophs and autotrophs in a fully oxygenated deep biofilm. Monod's intrinsic kinetics and Fickian diffusion were used for organic carbon uptake, while zero order intrinsic kinetics were assumed for both oxygen and nitrogen uptake. Nitrification was assumed to occur in the biofilm layer below the depth at which heterotrophic and nitrifying growth rates are equal. However, the fluid mass transfer resistance at the biofilm surface was neglected as well as the limitation of biofilm depth due to sloughing or immature growth. The model therefore has limited applicability.

Gonec and Harremoes [18] presented criteria for simultaneous organic oxidation and nitrification in a rotating disc system. Using the data available in the literature, they showed that the ratio between bulk soluble BOD_5 and oxygen concentration should be less than five to achieve nitrification (nitrification criterion). However, for simultaneous organic oxidation and nitrification in the system, the nitrification rate must be reduced compared to pure nitrification, namely the mixture and distribution of heterotrophs and nitrifiers within the biofilm, and oxygen penetration into the biofilm to allow the growth of nitrifiers.

Wanner and Gujer [19] presented a model to describe competition between several species in biofilms. The model depicted competition in biofilms between nitrifiers and heterotrophic bacteria that use a common nutrient (oxygen). By using a series of mass balances on organisms and substrates that incorporated diffusion and reaction in the biofilm, conversion to inert materials and sloughing of biomass, the model described competition at any layer in the biofilm. Computer simulations showed that nitrifiers will locate themselves in the biofilm only where conditions at the biofilm support surface (the media) are such that the heterotrophic and autotrophic growth rates are equal. The model also predicted that nitrifiers could compete successfully with heterotrophs only when the COD concentration was less than about 27 mg l^{-1}. The model addressed dynamic states and formed a steady state in which the biofilm thickness was assumed a priori. They made no attempt to predict steady state substrate fluxes, biofilm thickness and species distribution from the bulk liquid substrate concentration.

Chen et al. [20] developed a mathematical model for simultaneous removal of organic and nitrogen compounds in a rotating submerged disc reactor taking into account the relationships between carbon oxidation, nitrification and denitrification. Synthetic dual and triple Monod-type kinetics describing organic oxidation, nitrification and denitrification reactions were incorporated into the mass balance equations. The bulk liquid phase was assumed to be completely mixed. Further, it was assumed that every species of bacteria (oxidizing, nitrifying and denitrifying) exists uniformly in the whole biofilm and that the sum of all kinds of bacteria is regarded as one kind of biomass. The results showed that the DO concentration is one of the most important operating factors for the reactions of simultaneous removal. They concluded that simultaneous carbon and nitrogen removal in a biofilm reactor are interdependent and consequently are influenced by the bulk water quality.

2.2. *Shock loading studies*

Micro-organisms, probably the most versatile form of life, can adapt to a wide variety of environmental conditions. This adaptation is accomplished by the reorganization of their macromolecular structure, the induction and/or repression of enzyme systems, and the reallocation of material in the cellular metabolic pools. The biological treatment of domestic sewage may be considered as the most important practical example of a continuous non-steady state culture system. Flow and BOD concentration of domestic sewage usually peaks during mid-day and drops well below average at night. Likewise, some industrial operations produce load peaks on a cycle related to the work day. Other industries have irregular loads that depend on the schedule of batch operations. In almost all cases, design flow rate, concentration and load to a process occur rarely. The control of effluent concentration in the reactor is complicated by the non-linear and autocatalytic nature of the reaction.

The response of *perturbed* continuous flow activated sludge systems has been thoroughly investigated in the literature. Most investigators examined kinetic models and overall phenomenological characteristics of the transient reactors such as bulking, change in predominant species and nitrification efficiency etc. Most of these transient experiments have involved step or impulse inputs to the reactors. However, many influent variations are cyclic in nature and may therefore be approximated by sinusoidal forcing func-

tions. Sinusoidal disturbances have been applied to biological reactors in only a few cases. Zines and Rogers [21] studied ethanol inhibition in a nitrogen limited chemostat subjected to sinusoidal changes in dilution rate. Gilley and Bungay [22] measured the effect of sinusoidally varying dilution rates on growth rates of yeast and Westberg [23] investigated maintaining a constant effluent substrate concentration while a completely mixed activated sludge reactor was disturbed by sinusoidal variations in the influent.

Borzani et al. [24] studied the response of an aerobic culture to periodic variation of feed concentration at a very slow frequency, i.e. one cycle every 24 h. Cooney and Wang [25] studied the transient response of a chemostat under dual nutrient limitation following a pulse of one of the limiting nutrients.

As evident from the above discussion, most transient experiments have involved activated sludge processes and only a few studies have been reported in the literature to access the performance of an upflow packed bed biofilm reactor (UPBR), also known as submerged filter. It may be noted that UPBRs are finding extensive applications in wastewater treatment processes because of economic considerations and simplicity of operation. The active micro-organisms become attached to or are held by the supporting media in sufficient quantities to provide a long retention time, and the effluent suspended solids are well stabilized and consist largely of inert and settleable cell solids. Further, in a packed bed reactor the biological solids are reduced through endogenous respiration, thereby decreasing handling and treatment problems. Treatment of ammonia in a packed bed bioreactor by McHarness et al. [26], and efficient nitrification by Beg and Hassan [27,28], are some of the reported successful uses of upflow packed bed biofilm reactors.

Young and McCarty [29] were the first to model packed-bed biofilm reactors for wastewater treatment. Since then a number of models have been introduced in order to describe these reactors [30–33]. However, these models have shortcomings. One problem is the need to use zero or first order approximations for the Monod equation when developing a reactor model. These approximations are necessary because the use of the Monod equation in a diffusion-limited model results in a rate equation that cannot be solved analytically. The zero- and first-order models can be solved analytically but result in reactor models that are only accurate for very high or very low substrate concentrations. A more realistic biofilm model for a packed bed biofilm reactor was developed and presented by Beg and coworkers [34,35,27] by using the general axially dispersed plug flow model for both simple and loop packed-bed reactors. The performance characteristics of a packed-bed biofilm reactor for various reaction kinetics with and without substrate inhibition as well as the response of the reactor to various shock loads of feed concentration and temperature were also examined by them [36–38]. A biofilm model for simultaneous carbon oxidation and nitrification in an upflow packed bed biofilm reactor has also been developed [37]. Recently a number of attempts have been made to develop graphical techniques to evaluate the performance of packed and fluidized bed reactors as well as to develop approximate analytical solutions for biofilm models with Monod kinetics [39–42].

Manem and Rittmann [43] studied the effects of fluctuations in organic loading on the nitrification process and found that a sudden increase in organic loading led to temporary deterioration of nitrification efficiency and to the formation of nitrite. They employed step changes in organic loading and demonstrated that these fluctuations in input loading can adversely affect nitrification performance although long term nitrification is possible after establishment of a new steady-state. However, no attempt was made to study the oxygen utilization rates or when oxygen limitation may occur and affect substrate removal rates when simultaneous carbon oxidation and nitrification reactions are carried out. The objectives of the present study are, therefore, to investigate the possibility of oxygen limitation as well as the effect of sinusoidal variations of organic and ammonia concentrations on the performance of upflow packed bed biofilm reactors when simultaneous carbon oxidation and nitrification reactions are taking place.

3. Mathematical modeling

In the present model for simultaneous organic oxidation and nitrification, three substrates (organic carbon, NH_4^+–N and oxygen) are considered to be transported simultaneously

Table 1
Kinetic and mass transfer parameter values used in numerical computation

Parameter	Value	Reference
$\mu_{C\max}$ (25 °C)	2.315×10^{-4} s^{-1}	Watanabe et al. [44]
$\mu_{NH\max}$ (25 °C)	1.099×10^{-5} s^{-1}	Watanabe et al. [44]
Y_C	0.37	Watanabe et al. [44]
Y_{NH}	0.1	Watanabe et al. [44]
X_C	5.0×10^{4} mg dm^{-3}	Watanabe et al. [44]
X_{NH}	3.9×10^{4} mg dm^{-3}	Watanabe et al. [44]
K_C	20 mg dm^{-3}	Watanabe et al. [44]
K_{NH}	0.5 mg dm^{-3}	Watanabe et al. [44]
$K_{O\text{-}C}$	0.5 mg dm^{-3}	Watanabe et al. [44]
$K_{O\text{-}NH}$	2.5 mg dm^{-3}	Watanabe et al. [44]
A_C	0.75	Watanabe et al. [44]
A_{NH}	4.33	Watanabe et al. [44]
D_C	2.083×10^{-5} cm^2 s^{-1}	Watanabe et al. [44]
D_{NH}	2.546×10^{-5} cm^2 s^{-1}	Watanabe et al. [44]
D_O	2.893×10^{-5} cm^2 s^{-1}	Watanabe et al. [44]
L	240 cm	Hassan and Beg [35]
u	0.8 cm s^{-1}	Hassan and Beg [35]
ϵ	0.4	Hassan and Beg [35]
S_{NH0}	200 mg dm^{-3}	
S_{C0}	50 mg dm^{-3}	
a	160 cm^2 cm^{-3}	Hassan and Beg [35]
Pe_i	100	Hassan and Beg [35]
L_c	0.05 cm	Hassan and Beg [35]
k_{LC}	1.835×10^{-4} cm s^{-1}	Grady and Lim [45]
$k_{L,NH}$	2.061×10^{-4} cm s^{-1}	Grady and Lim [45]
k_{LO}	2.220×10^{-4} cm s^{-1}	Grady and Lim [45]

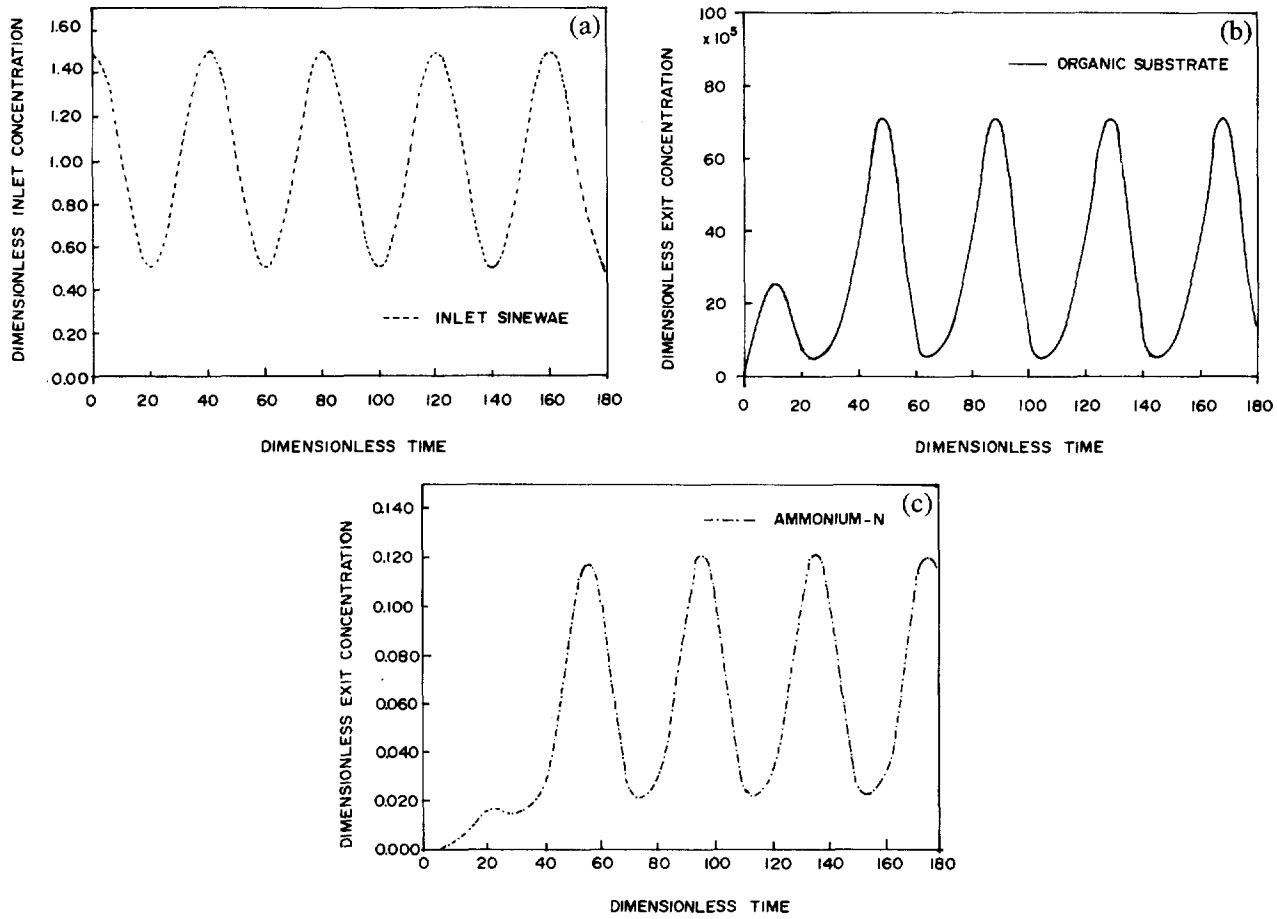

Fig. 1. (a) Inlet perturbation for methanol feed concentration and dynamic response of (b) methanol exit concentration, (c) NH_4^+–N exit concentration ($A^* = 0.5$, $CT^* = 40.0$, $S_{NH0} = 200$ mg l^{-1}, $S_{C0} = 50$ mg l^{-1}, temperature 25 °C).

from the bulk liquid phase through the external film on to the surface of the biofilm, followed by diffusion and reaction within the biofilm. Dual Monod interactive kinetics for both carbon oxidation and nitrification are used.

The following assumptions have been made in obtaining the appropriate equations for the present system.

1. The biofilm is homogeneous with regard to biofilm density and the bioreactor operates at pseudo-steady state so that the biofilm properties such as biofilm thickness and density are constant.
2. NH_4^+–N, oxygen and organic substrate are considered as growth limiting and all other nutrients are provided in excess.
3. There are no physiological changes when organisms are immobilized on the solid support surface. Thus, the kinetic expression for cell growth and substrate degradation obtained from freely suspended cell culture can be used.
4. The kinetics of growth in the biofilm based on methanol (organic carbon source), NH_4^+–N and oxygen concentrations are assumed to be governed by the following equations:for carbon oxidation,

$$\mu = \frac{\mu_{Cmax} S_{Cf}}{K_C + S_{Cf}} \frac{S_{Of}}{K_{OC} + S_{Of}} \tag{1}$$

for nitrification,

$$\mu = \frac{\mu_{NHmax} S_{NHf}}{K_{NH} + S_{NHf}} \frac{S_{Of}}{K_{ONH} + S_{Of}} \tag{2}$$

5. The bulk flow is approximated by the axial dispersion model.
6. Within the biofilm, transport of chemical species may be described by molecular diffusion according to Fick's first law in one dimension (depth of biofilm) only.
7. The thickness of the biofilm is small compared to characteristic dimensions of the packing and hence a flat plate geometry can be assumed.
8. Charged molecules are not subjected to interactions with the biomass matrix.

The reactor configuration requires the general mass balance equation to be applied for a control volume of liquid within the reactor and biofilm:

Accumulation = Input − Output − Removal by reaction

We therefore obtain for the biofilm phase, for any substrate i,

$$\frac{\partial S_{fi}}{\partial t} = D_{ci} \frac{\partial^2 S_{fi}}{\partial y^2} - r[S_i, S_j] \quad (i = 1,2,\ldots n, j = 2) \tag{3}$$

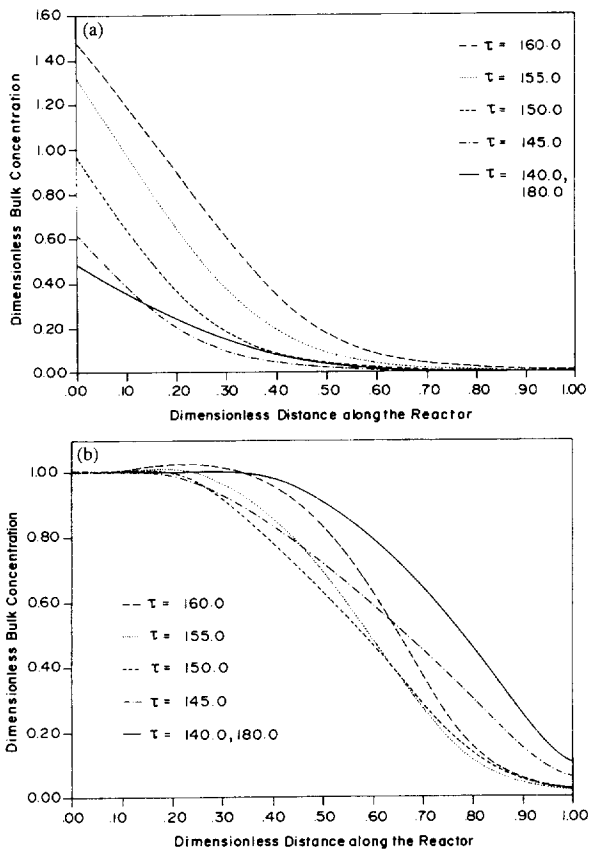

Fig. 2. Bulk concentration profiles of (a) NH_4^+–N and (b) methanol as a function of dimensionless reactor length ξ, at various dimensionless times; methanol sinusoidal perturbation, $S_{NH0}=200$ mg l^{-1}, $S_{CO}=50$ mg l^{-1}.

where, $i=1$ = ammonium–N, $i=2$ = oxygen, $i=3$ = organic substrate (methanol in this study) with the boundary conditions,

$$y=0 \quad D_{ci}\left.\frac{\partial S_{fi}}{\partial y}\right|_{y=0} = -k_{Li}(S_i - S_{fi}|_{y=0}) \tag{4}$$

and

$$y=L_c \quad D_{ci}\left.\frac{\partial S_{fi}}{\partial y}\right|_{y=0} = 0 \tag{5}$$

the corresponding initial condition is,

$$y\geq 0 \quad t=0 \quad S_{fi}=S_{fi}^0 \tag{6}$$

For the external fluid phase, the flow behaviour is characterized by an axial dispersed plug flow model. The equation for the external phase may therefore be written as,

$$\epsilon\frac{\partial S_i}{\partial t} = D_{ei}\frac{\partial^2 S_i}{\partial z^2} - u\frac{\partial S_i}{\partial z} - k_L a[S_i - S_{fi}|_{y=0}] \tag{7}$$

The corresponding boundary conditions are written as

$$z=0 \quad D_{ei}\left.\frac{\partial S_i}{\partial z}\right|_{z=0^+} = -u[S_i|_{z=0^-} - S_i|_{z=0^+}] \tag{8}$$

and

$$z=L \left.\frac{\partial S_i}{\partial z}\right|_{z=L} = 0 \tag{9}$$

where $S|_{z=0^-}$ is the concentration of substrate at the inlet of the reactor

$$S|_{z=0^-} = S_i + A\sin[\pi(t+CT/2)/CT] \tag{10}$$

and the initial condition,

$$y\geq 0 \quad t=0 \quad S_i=S_i^0 \tag{11}$$

The concentration of oxygen is assumed to remain constant at its saturation value, i.e. 8 mg l^{-1} in the bulk liquid phase throughout the length of the reactor.

Eqs. 3-11 can be reduced to the dimensionless form, by the introduction of the following parameters:

$$SF_i^* = S_{fi}/S_{i0} \quad S_i^* = S_i/S_{i0} \quad Bi_i = k_{Li}L_c/D_c$$
$$\xi = z/L \quad \eta = y/L_c \quad Pe_i = Lu/D_{ei}$$
$$\alpha_i = k_{Li}aL/u \quad \tau = ut/L\epsilon \quad \beta_i = D_{ci}L\epsilon/L_c^2 u$$

In the dimensionless form, Eqs. 3-11 then become,

$$\frac{\partial S_{fi}^*}{\partial \tau} = \beta_i\frac{\partial^2 S_{fi}^*}{\partial \eta^2} - \langle R(S_i,S_j)\rangle \tag{12}$$

with the boundary conditions:

$$\text{at } \eta=0 \quad \left.\frac{\partial S_{fi}^*}{\partial \eta}\right|_{\eta=0} = -Bi_i[S_i^* - S_{fi}^*|_{\eta=0}] \tag{13}$$

and

$$\text{at } \eta=1 \quad \left.\frac{\partial S_{fi}^*}{\partial \eta}\right|_{\eta=1} = 0 \tag{14}$$

the initial condition,

$$\eta\geq 0 \quad \tau=0 \quad S_{fi}=S_{fi}^0 \tag{15}$$

For the external fluid phase,

$$\frac{\partial S_i^*}{\partial \tau} = \frac{1}{Pe_i}\frac{\partial^2 S_i^*}{\partial \xi^2} - \frac{\partial S_i^*}{\partial \xi} - \alpha_i[S_i^* - S_{fi}^*|_{\eta=0}] \tag{16}$$

with the boundary conditions

$$\xi=0 \quad \left.\frac{\partial S_i^*}{\partial \xi}\right|_{\xi=0^+} = -Pe_i[S_i^*|_{\xi=0^-} - S_i^*|_{\xi=0^+}] \tag{17}$$

and

$$\xi=1 \quad \left.\frac{\partial S_i^*}{\partial \xi}\right|_{\xi=1} = 0 \tag{18}$$

with the initial condition,

$$\xi\geq 0 \quad \tau=0 \quad S_i^*=S_{i0}^* \tag{19}$$

The inlet concentration has been varied sinusoidally according to the relations

$$S^*|_{\xi=0^-} \equiv Chz = 1.0 + A_{mp}^*\sin[\pi(\tau+CT^*/2)/CT^*] \tag{20}$$

The dimensionless reaction terms $\langle R(S_i,S_j)\rangle$ consist of inter-

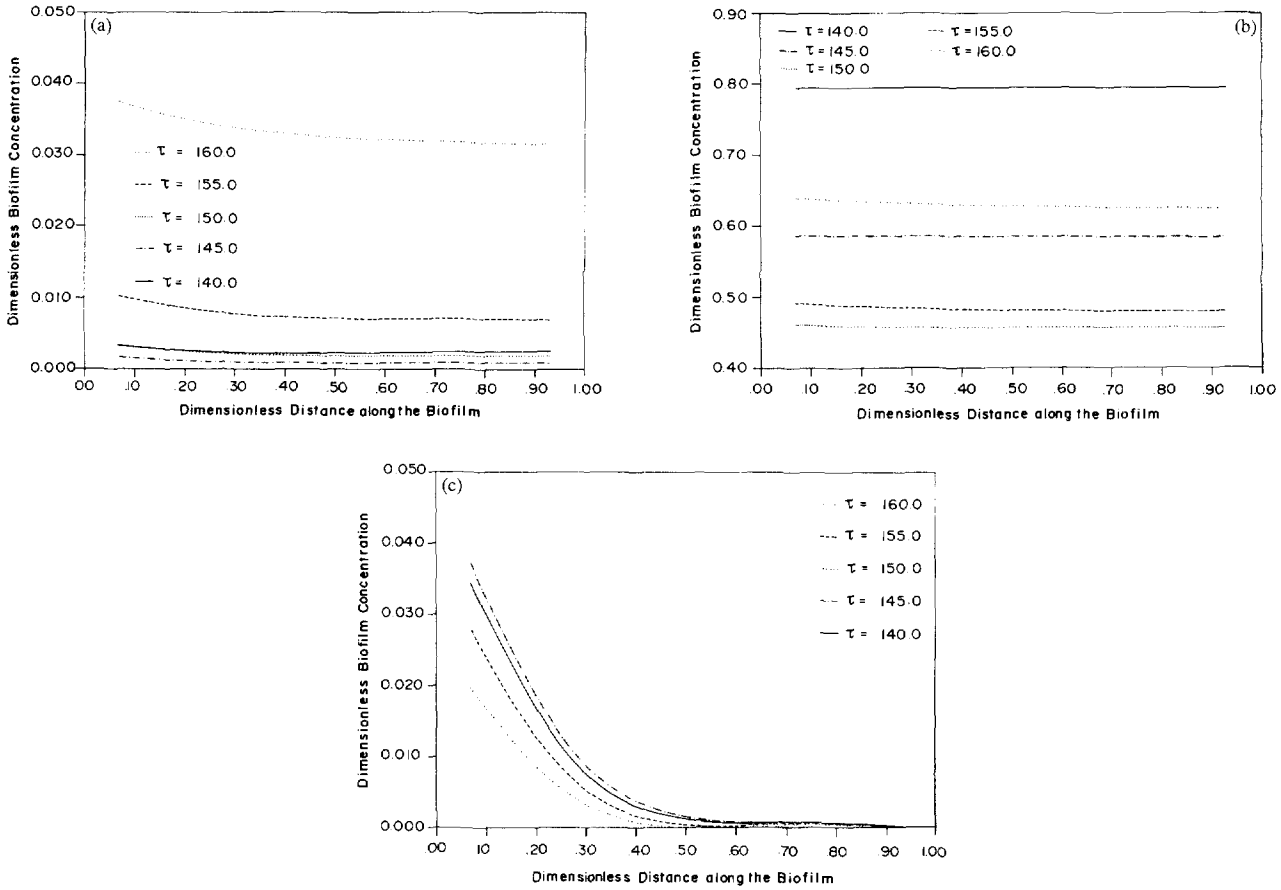

Fig. 3. Concentration profiles of (a) methanol, (b) NH_4^+–N and (c) oxygen in the biofilm at various dimensionless times; methanol sinusoidal perturbation, $S_{NH0}=200$ mg l^{-1}, $S_{C0}=25$ mg l^{-1}, $\xi=0.5$.

active Michaelis–Menten kinetics modified for a dual-substrate system:For organic substrate (methanol)

$$R_C=\frac{L\epsilon\mu_{C\max}X_C}{Y_C u S_{C0}}\left[\frac{SF_C^*}{K_C+SF_C^*}\right]\left[\frac{SF_O^*}{K_{O-C}+SF_O^*}\right] \quad (21)$$

for NH_4^+–N,

$$R_{NH}=\frac{L\epsilon\mu_{NH\max}X_{NH}}{Y_{NH}uS_{NH0}}\left[\frac{SF_{NH}^*}{K_{NH}+SF_{NH}^*}\right]\left[\frac{SF_{NH}^*}{K_{O-NH}+SF_{NH}^*}\right] \quad (22)$$

For oxygen,

$$R_O=-A_{NH}R_{NH}-A_CR_C \quad (23)$$

The above set of normalized Eqs. 12-19 has been solved by the method of orthogonal collocation from the transient to the steady state conditions. The solution procedure has been described in detail by Hassan and Beg [35].

4. Results and discussion

The performance of an upflow packed bed biofilm reactor was analysed when subjected to sinusoidal variation of feed concentrations by means of numerical simulations. The carbon oxidation accompanied by nitrification was chosen as the model reaction system because of obvious environmental significance. NH_4^+–N was considered as nitrogen source while organic substrate, methanol, was chosen as carbon source. The numerical solution of the proposed equations defining the system was obtained for a wide range of operating conditions. The values of basic parameters used in numerical computations are given in Table 1. The inlet concentrations of the two substrates were selected on the basis of values available in the literature for high strength wastes encountered in practice [46–49].

Fig. 1(a) shows the inlet perturbation of organic substrate, methanol, concentration and Fig. 1(b,c) shows the corresponding response of the system in terms of its approach to steady state conditions. The exit concentration of NH_4^+–N takes a little longer to reach the cyclic steady state ($\tau=60$) compared to the methanol exit concentration ($\tau=50$). It is interesting to note that the exit concentration of NH_4^+–N also follows a sinusoidal pattern although its inlet concentration was subjected to step input. It may also be observed by comparing the inlet forcing functions with both the NH_4^+–N and methanol exit concentrations that their responses are synchronized with the disturbance, however, the time lag for the NH_4^+–N exit concentration is twice ($\tau=18$) that of the organic substrate ($\tau=9$). This implies that the peak in inlet

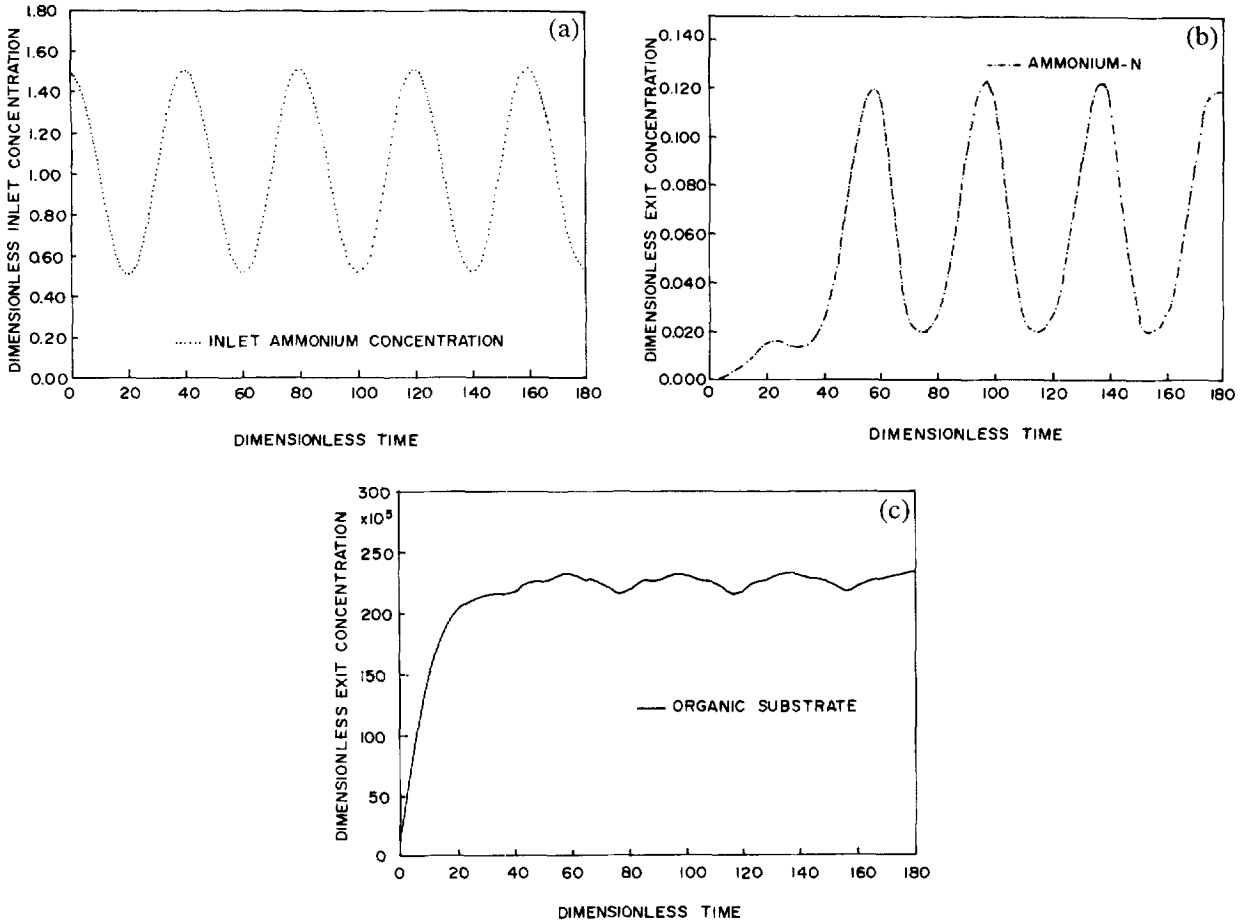

Fig. 4. (a) Inlet perturbation for NH_4^+–N feed concentration and dynamic response of (b) NH_4^+–N exit concentration, (c) methanol exit concentration ($A^* = 0.5$, $CT^* = 40.0$, $S_{NH0} = 200$ mg l^{-1}, $S_{C0} = 50$ mg l^{-1}, temperature 25 °C).

disturbance corresponds to a dip in the NH_4^+–N exit concentration. The organic oxidation and nitrification reactions are interrelated through dissolved oxygen utilization. When the inlet organic concentration attains its maximum value, most of the dissolved oxygen is utilized for organic oxidation leaving very little dissolved oxygen for significant nitrification to take place.

Fig. 2(a,b) shows the variation of bulk profiles of NH_4^+–N and methanol in the bed as a function of dimensionless distance along the length of the reactor at various times during a complete cycle at cyclic steady state conditions. It may be observed that in the region $\xi < 0.2$, there is very little nitrification taking place while methanol depletes at a high rate. For $\xi > 0.8$, no significant organic oxidation occurs while nitrification continues to take place. However, in the region $0.2 < \xi < 0.8$, the rate of nitrification increases while a decrease in oxidation rate of methanol is observed. For $\xi > 0.8$, owing to almost complete oxidation of methanol the nitrification is the dominant reaction. This may be explained on the basis of microbial competition between heterotrophs and nitrifiers. Nitrifiers, being the slower growing organisms of the two, could only compete with heterotrophs for dissolved oxygen in the biofilm after substantial organic oxidation has taken place.

The concentration profiles of methanol, NH_4^+–N and oxygen in the biofilm as a function of dimensionless time at the centre of the bed are shown in Fig. 3(a–c) respectively. As can be seen, the concentration profiles of methanol and NH_4^+–N within the biofilm are flat implying that the internal diffusion resistance for these compounds is negligible. However, the corresponding profiles of oxygen show a significant variation as a result of significant diffusional resistance as depicted in Fig. 3(c). It may further be noted that at the middle of the reactor, oxygen becomes the limiting substrate since its concentration drops very close to zero beyond a film thickness of $\eta = 0.6$.

The effect of sinusoidal variation of NH_4^+–N inlet concentration on the system response was also investigated. This will enable identification of the substrate whose inlet concentration variation has a profound effect on the performance of the system.

Fig. 4(a) shows the inlet NH_4^+–N disturbance and Fig. 4(b,c) shows the corresponding response of the system in terms of dimensionless exit concentrations of NH_4^+–N and methanol respectively. The exit NH_4^+–N concentration lags the input disturbance by $\tau = 18$. The inlet methanol concentration was subjected to a step input. The response of the methanol exit concentration has not been significantly

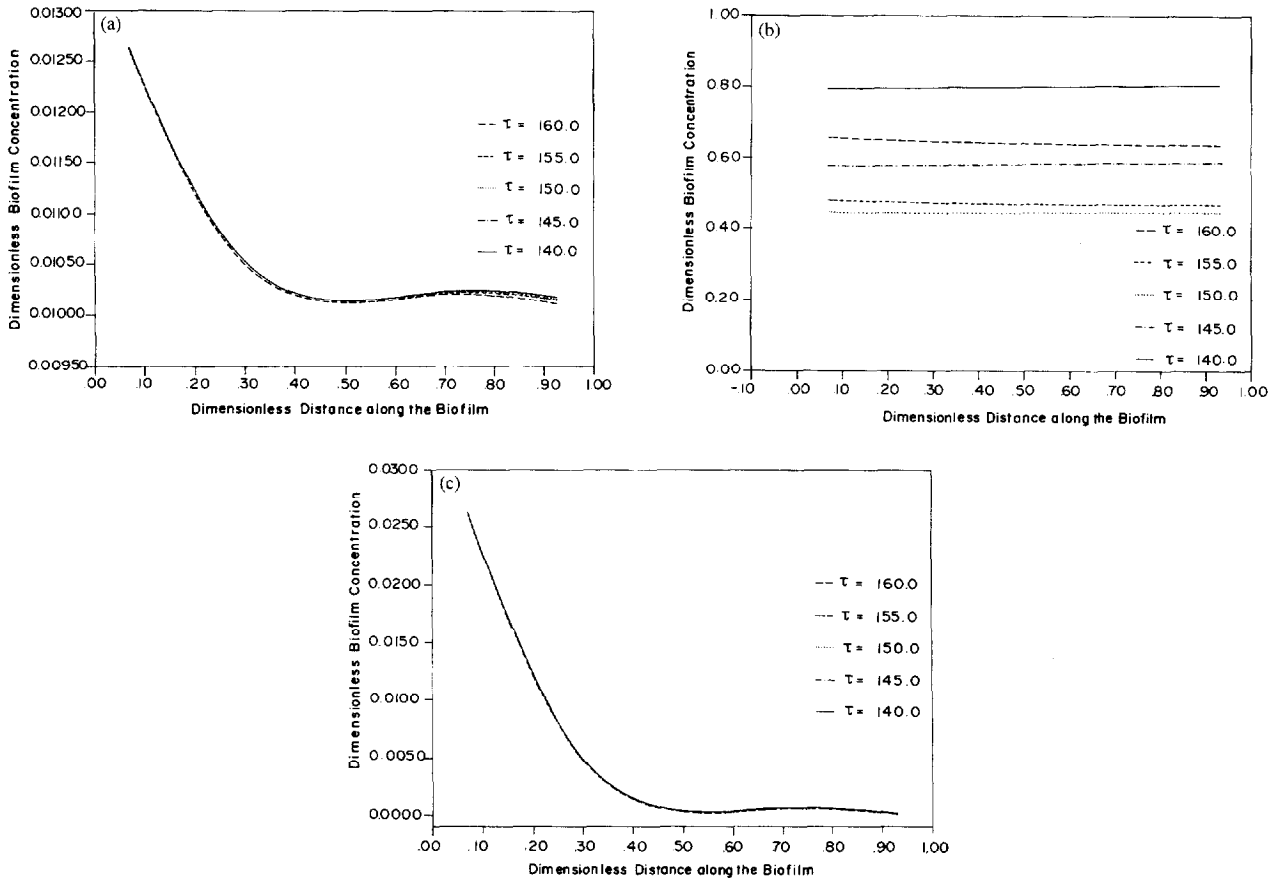

Fig. 5. Concentration profiles of (a) methanol, (b) NH_4^+–N and (c) oxygen in the biofilm at various dimensionless times; NH_4^+–N sinusoidal perturbation, $S_{NH0} = 200$ mg l^{-1}, $S_{C0} = 25$ mg l^{-1}, $\xi = 0.5$.

affected by sinusoidal variation of the inlet NH_4^+–N concentration. This is in sharp contrast to the case previously considered where the inlet methanol concentration was changed sinusoidally and the exit NH_4^+–N concentration was found to follow a sinusoidal pattern of variation. This can be attributed to the essentially complete consumption of methanol and therefore the effect of NH_4^+–N perturbation becomes less pronounced on the relatively low available concentration of methanol.

The variations of biofilm concentrations of methanol, NH_4^+–N and oxygen with time at the centre of the bed are shown in Fig. 5(a–c) respectively. As evident from Fig. 5(a,c), the variation of biofilm oxygen concentration again follows the organic substrate concentration variation. Oxygen is also the limiting substrate under the conditions considered.

5. Conclusions

Numerical simulation has been performed to analyse the performance of an upflow packed bed biofilm reactor under multi-substrate limitation involving simultaneous carbon oxidation and nitrification reactions. The numerical solution of the proposed model equations defining the system has been obtained for a wide range of operating conditions to ensure individual substrate limitation behaviour. For an inlet concentration of 200 mg l^{-1} of NH_4^+–N and 50 mg l^{-1} of organic substrate (methanol), the results show the methanol is consumed in the first half of the reactor while most of the NH_4^+–N is converted in the latter half of the bed. The sinusoidal variation of organic substrate concentration has a much more profound effect on the system response compared to the sinusoidal variation of inlet NH_4^+–N concentration. When the inlet concentration of methanol is subjected to sinusoidal variation, the exit concentration of NH_4^+–N also follows a sinusoidal pattern although its inlet concentration was subjected to step input. It may therefore be concluded from this simulation study that a sufficient oxygen supply should be maintained near the reactor inlet as most of the organic substrate may be consumed in that part of the reactor.

Acknowledgements

The authors wish to acknowledged the support provided by the King Fahd University of Petroleum and Minerals, Dhahran, Saudi Arabia.

Appendix A. Nomenclature

a surface area of biofilm per unit volume of bed (cm^{-1})
A^*_{mp} amplitude of the sine wave (—)
A_C oxygen requirement in organic oxidation (—)
A_{mp} amplitude of the sine wave ($mg\ l^{-1}$)
A_{NH} oxygen requirement in nitrification (—)
Bi_i Biot number for substrate i (—)
CT cycle time (frequency) of the sine wave (cycle min^{-1})
CT* cycle time (frequency) of the sine wave (—)
D_{Ci} molecular diffusivity of substrate i in the biofilm ($cm^2\ s^{-1}$)
$i=1$ = ammonium–N
$i=2$ = oxygen
$i=3$ = organic substrate (methanol, in this study)
D_{ei} dispersion coefficient of substrate i ($cm^2\ s^{-1}$)
k_C Michaelis constant for organic substrate (methanol) ($mg\ l^{-1}$)
K_C Michaelis constant for organic substrate (methanol) (—)
k_{Li} mass transfer coefficient of substrate i ($cm\ s^{-1}$)
k_{NH} Michaelis constant for ammonium–N ($mg\ l^{-1}$)
K_{NH} Michaelis constant for ammonium–N (—)
$k_{O\text{-}C}$ Michaelis constant of oxygen in organic oxidation ($mg\ l^{-1}$)
$K_{O\text{-}C}$ Michaelis constant of oxygen in organic oxidation (—)
$k_{O\text{-}NH}$ Michaelis constant of oxygen in nitrification ($mg\ l^{-1}$)
$K_{O\text{-}NH}$ Michaelis constant of oxygen in nitrification (—)
L length of reactor (cm)
L_c biofilm thickness (cm)
Pe_i Peclet number (—)
S_{Cf} biofilm methanol concentration ($mg\ l^{-1}$)
S_{C0} inlet organic substrate concentration ($mg\ l^{-1}$)
S_{fi} concentration of substrate i inside biofilm ($mg\ l^{-1}$)
S^*_{fi} concentration of substrate i inside biofilm (—)
S_i concentration of substrate i in the bulk liquid ($mg\ l^{-1}$)
S^*_i concentration of substrate i in the bulk liquid (—)
S_{NHf} biofilm ammonium–N concentration ($mg\ l^{-1}$)
S_{NH0} inlet ammonium–N concentration ($mg\ l^{-1}$)
S_{Of} biofilm oxygen concentration ($mg\ l^{-1}$)
t reaction time (s)
u velocity of the bulk liquid ($cm\ s^{-1}$)
X_C concentration of heterotrophs in the biofilm ($mg\ l^{-1}$)
X_{NH} concentration of nitrifiers in the biofilm ($mg\ l^{-1}$)
y coordinate for biofilm (cm)
Y_C yield coefficient of heterotrophs (—)
Y_{NH} yield coefficient of nitrifiers (—)
z axial coordinate for reactor (cm)

Greek letters

μ_{Cmax} maximum specific growth rate of heterotrophs (s^{-1})
μ_{NHmax} maximum specific growth rate of nitrifiers (s^{-1})
τ time (—)
α_i mass transfer parameter (Stanton number) of substrate i (—)
ϵ bed void fraction of reactor (—)
η coordinate for biofilm (—)
β_i dimensionless diffusion coefficient of substrate i

References

[1] B. Sharma, R.C. Ahlert, Water Res. 11 (1977) 897–925.
[2] D. Barnes, P.J. Bliss, Biological Control of Nitrogen in Wastewater Treatment, E.&F. Spon, London, 1983.
[3] D.O. Focht, A. Chang, Adv. Appl. Microbiol. 19 (1975) 153–156.
[4] E.L. Schmidt, Nitrification in soil, in: R.C. Dinauer, K.E. Gates, M. Stelly, F.J. Stevanson, J.M. Bremner, R.D. Hauck, D.R. Keeney (eds.), Nitrogen in Agricultural Soils, Agronomy, Madison, WI, 1982, pp. 253–288.
[5] H.A. Painter, Nitrification in the treatment of sewage and wastewaters, in: J.I. Prosser (ed.), Nitrification, IRL Press, Oxford, 1986, pp. 185–211.
[6] H.A. Painter, Water Res. 4 (1970) 393–450.
[7] J.G. Kuenen, L.A. Robertson, Ecology of nitrification and denitrification, Symposium Soc. Gen. Microbiol., 42nd nitrogen sulphur cycles, 1988, pp. 161–218.
[8] M.I.H. Aleem, Ann. Rev. Plant Physiol. 21 (1970) 67–90.
[9] W. Wallace, D.J.O. Nicholas, Biol. Rev. 44 (1969) 359–391.
[10] H. Odegaard, B. Rusten, Nitrogen removal in RBC without use of external carbon source, Paper presented at the 1st National Symposium Workshop on RBC t-echnology, University of Pittsburg, PA, 1980.
[11] K.L. Murphy, P.M. Sutton, R.W. Wilson, B.E. Jank, J. Water Poll. Control Fed. 49 (1977) 549–557.
[12] O. Hao, G.F. Hendricks, Water Sewage Works 122 (1975) 48–50, 70–73.
[13] P.M. Crawford, Use of RBC for nitrification at the city of Guleph WPC plant, Paper presented at the 1st National Symposium Workshop on RBC Technology, University of Pittsburg, PA, 1980.
[14] R.L. Antonie, Water Sewage Works 121 (1974) 44–46, 54–56.
[15] W.H. Torpey, H. Heukelekian, A.J. Kaplovsky, L. Epstein, Effect of exposing slimes on rotating discs to atmospheres enriched with oxygen, Proc. 6th Industrial Waste Conference on WPR, 1972, pp. 405–417.
[16] P. Harremoes, Water Sci. Technol. 14 (1982) 167–187.
[17] S.E. Strand, J. Environ. Eng. 112 (1986) 785–804.
[18] E. Gonec, P. Harremoes, Water Res. 24 (1990) 499–505.
[19] O. Wanner, W. Gujer, Water Sci. Technol. 17 (1984) 27–44.
[20] G.H. Chen, H. Ozaki, Y. Terashima, Water Sci. Technol. 21 (1989) 791–804.
[21] D.O. Zines, P.L. Rogers, Biotech. Bioeng. 13 (1971) 293–308.
[22] J.W. Gilley, H.R. Bungay, Biotech. Bioeng. 9 (1967) 617–621.
[23] N. Westberg, Water Res. 3 (1969) 613–621.
[24] W. Borzani, R.E. Gregori, M.L.R. Vairo, Biotech. Bioeng. 18 (1976) 623–632.
[25] C.L. Cooney, D.I.C. Wang, Biotech. Bioeng. 18 (1976) 189–198.
[26] D.D. McHarness, R.T. Haug, P.L. McCarty, J. Water Poll. Control Fed. 47 (1975) 291–304.
[27] S.A. Beg, M.M. Hassan, Chem. Eng. J. 30 (1985) B1–B8.
[28] S.A. Beg, M.M. Hassan, Water Res. 21 (1987) 191–198.

[29] J.C. Young, P.L. McCarty, J. Water Poll. Control Fed. 41 (1969) R160–R173.
[30] A.D. Meunier, K.J. Williamson, J. Environ. Eng. Div. ASCE 107 (1981) 307–317.
[31] C.T. Skowlund, D.W. Kirmse, Biotech. Bioeng. 33 (1989) 164–172.
[32] P.A. Jennings, V.L. Snoeyink, E.S.K. Chain, Biotech. Bioeng. 18 (1976) 1249–1273.
[33] P. Harremoes, J. Water Poll. Control Fed. 48 (1976) 377–387.
[34] M. Atiqullah, M.M. Hassan, S.A. Beg, Chem. Eng. J. 44 (1990) B57–B67.
[35] M.M. Hassan, S.A. Beg, Chem. Eng. J. 36 (1987) B15–B27.
[36] S.A. Beg, M.M. Hassan, M.A.S. Chaudhry, Int. J. Environ. Studies 49 (1995) 31–52.
[37] S.A. Beg, M.M. Hassan, M.A.S. Chaudhry, J. Chem. Tech. Biotechnol. 64 (1995) 367–378.
[38] S.A. Beg, M.M. Hassan, M.A.S. Chaudhry, Chem. Eng. Technol. 19 (1996) 43–49.
[39] B.R. Kim, M.T. Suidan, Water Res. 23 (1989) 1491–1498.
[40] G.V. Bhaskar, S.M.R. Bhamidimarri, Can. J. Chem. Eng. 69 (1991) 544–547.
[41] M.T. Suidan, Y.T. Wang, B.R. Kim, Water Res. 23 (1989) 837–844.
[42] P.S. Golla, T.J. Overcamp, J. Environ. Eng. 116 (1990) 829–836.
[43] J.A. Manem, B.E. Rittmann, J. AWWA 84 (1992) 147–151.
[44] Y. Watanabe, S. Masuda, M. Ishiguro, Water Sci. Technol. 26 (1992) 511–522.
[45] C.P.L. Grady, H.C. Lim, Biological Wastewater Treatment: Theory and Applications, Marcel Dekker, New York, 1980.
[46] G.M. Wong-Chong, R.C. Loehr, AIChE Symp. Ser. 71 (1975) 70–79.
[47] R. Srna, A. Baggaley, J. Water Poll. Control Fed. 47 (1975) 472–486.
[48] T.B.S. Prakasam, R.C. Loehr, Water Res. 6 (1972) 859–869.
[49] T.B.S. Prakasam, Y.D. Joo, E.G. Srinath, R.C. Loehr, Proc. 29th Ind. Waste Conf., Purdue University, 1974, pp. 497–509.